

C. E. Hadden\*, P. B. Bowman, W. H. Duholke, J. E. Guido, B. D. Kaluzny, R. H. Robins, D. J. Russell, S. M. Sims, T. J. Thamann and G. E. Martin

Pharmaceutical Development, Pharmacia and Upjohn, Kalamazoo, MI 49001-0199

Received March 10, 2000

The structures of the major thermal degradation products of linezolid (Zyvox<sup>®</sup>, PNU-100766) are reported. Following hydrolytic decarboxylation, the remaining oxazolidinone-derived skeleton of the antibiotic underwent a variety of acetyl migrations prior to deacetylation. Three of the degradation products are structural isomers. Structural characterization of the degradants was accomplished *via* the concerted analysis of 2D NMR, mass spectrometric, and infrared data. Direct and long-range  $^1\text{H}$ - $^{15}\text{N}$  heteronuclear shift correlation experiments at natural abundance were performed on linezolid as well as each of the isolated products of the degradation cascade.  $^{15}\text{N}$  chemical shifts for linezolid and each of the degradants, as well as the observed long-range  $^1\text{H}$ - $^{15}\text{N}$  coupling pathways are reported.

*J. Heterocyclic Chem.*, **37**, 1623 (2000).

### Introduction.

Linezolid (Zyvox<sup>®</sup>, **1**) is a first generation oxazolidinone for the treatment of infectious diseases caused by susceptible and resistant strains of *Staphylococcus aureus*, *Streptococcus pneumoniae*, *Enterococcus* species, and other Gram positive organisms.

To comply with FDA and ICH regulatory submission requirements, linezolid was subjected to various stress challenges to assess the stability of the drug. The present study was directed at the structural characterization of degradation products formed during thermal stability challenges on aqueous solutions of the drug. The structures of the thermally-induced degradation products were characterized by conventional spectroscopic means as well as by long-range  $^1\text{H}$ - $^{15}\text{N}$  heteronuclear shift correlation methods at natural abundance.  $^{15}\text{N}$  chemical shift data provided a convenient means of unequivocal location of the acetyl moiety.

The primary degradation products formed from thermally stressed aqueous solutions of linezolid were the amides **2** and **4**. These degradants can readily arise following the hydrolytic decarboxylation of the oxazolidinone ring. The degradant formed directly from ring scission is the N-7 acetyl structure shown by **2**. Acetyl migration, presumably *via* the intermediate perhydro-pyrimidine, **3**, would afford the N-3 acetyl degradant structure shown by **4** (see Scheme 1). Details of the kinetics of the thermal degradation cascade will be reported elsewhere. Acetyl migration *via* either of the intermediates, **5** or **6**, could lead to the formation of the O-5 acetyl degradant structure shown by **7**. It was found that **7** was formed only in degraded samples of **4**, but it is possible that both potential pathways through intermediates **5** and **6** are involved in the formation of **7**. It is clear that **7** was not one of the major thermal degradants of linezolid. Any or potentially all of the three isolable acetyl products of the thermal degradation cascade, **2**, **4**, or **7**, can presumably undergo deacetylation to afford the final product of the cascade, **8**.

### Results and Discussion.

Elucidation of the degradation product structures was straight-forward using conventional spectroscopic methods. The only potential point of ambiguity would be the nitrogen, N-3 vs. N-7, on which the acetyl moiety resided in a particular structure. The acquisition of long-range  $^1\text{H}$ - $^{15}\text{N}$  GHMBC [1] data was undertaken to begin to establish a database that could be used to irrefutably differentiate between the *N*-acetyl structures. The long-range coupling pathways observed for linezolid and its degradants also help to broaden the database of long-range  $^1\text{H}$ - $^{15}\text{N}$  couplings available to chemists faced with the challenge of assembling the structure of an unknown. The  $^{15}\text{N}$  chemical shift assignments for **1**, **2**, **4**, **7**, and **8** are collected in Table 1.

Table 1

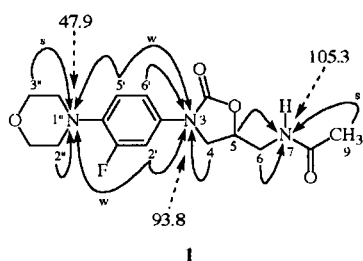
The  $^{15}\text{N}$  chemical shifts for the degradation cascade of the antibiotic linezolid (**1**), referenced to external liquid ammonia.

	<b>1</b>	<b>2</b>	<b>4</b>	<b>7</b>	<b>8</b>
Position	$^{15}\text{N}$ Chemical Shift				
3	93.8	56.7	109.1	53.8	54.9
7	105.3	109.5	23.9	23.7	22.0
1''	47.9	43.1	50.3	43.5	43.0

### Linezolid.

The structure of the oxazolidinone antibiotic linezolid (Zyvox) is shown by **1**. The 4-phenyl morpholine nitrogen was observed to resonate at 47.9 ppm, 12 ppm upfield of a normal *N*-phenyl morpholine. The upfield shift relative to *N*-phenyl morpholine can presumably be attributed to the fluoro substitution of the benzene ring. The oxazolidinone ring nitrogen resonated at 93.8 ppm, consistent with its carbamate nature; the terminal *N*-acetyl nitrogen resonated at 105.3 ppm. These

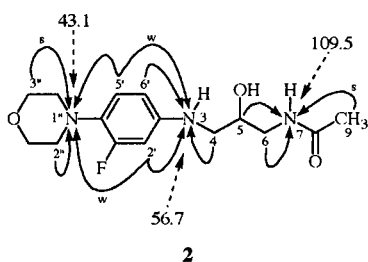
chemical shifts are consistent with those reported by us previously for the related oxazolidinone antibiotic eperezolid [2], in which the corresponding nitrogen resonances were observed at 52.3, 98.1, and 109.3 ppm, respectively. Eperezolid differs from linezolid in that the morpholine ring of linezolid is replaced by a 4-*N*-hydroxyacetyl piperazine, the acetylated piperazine nitrogen of eperezolid resonated at 111.0 ppm.



The long-range correlations for linezolid are shown by **1**. Strong and weak correlations are denoted by an (s) or (w), respectively. All expected correlations are observed. The strongest correlations were from the acetyl methyl group and the morpholino methylene. The two observed weak responses were four-bond couplings correlating H-2'-N-1'', and H-5'-N-3.

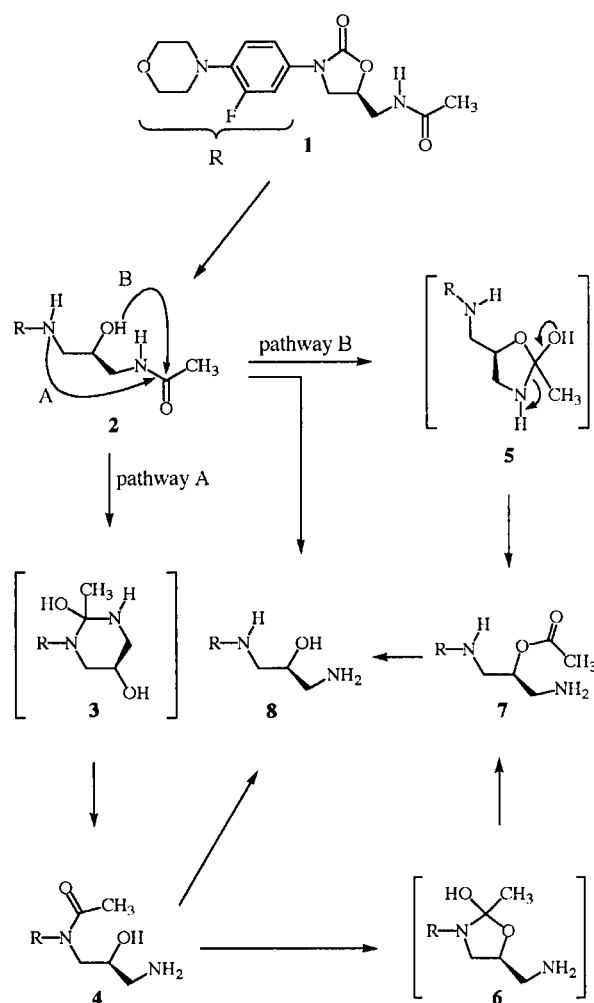
#### 7-*N*-Acetyl Degradant (2).

As noted above, the first thermally-induced degradant of linezolid is the hydrolytic decarboxylation product, **2**. The proton reference spectrum of **2** was characterized by the observation of the NH and OH resonances at 5.36 and 4.91 ppm, respectively.



The morpholine nitrogen resonated at 43.1 ppm, an upfield shift of -4.8 ppm relative to linezolid (**1**). We attribute the upfield shift of the morpholine nitrogen resonance to electronic effects transmitted through the  $\pi$  electrons of the benzene ring arising from the cleavage of the oxazolidinone ring. The N-3 amine nitrogen, previously part of the oxazolidinone ring, resonated at 56.7 ppm. The 37.1 ppm upfield shift is consistent with the hydrolytic decarboxylation of the oxazolidinone ring and the conversion of the N-3 carbamate nitrogen of **1**, to the

Scheme 1



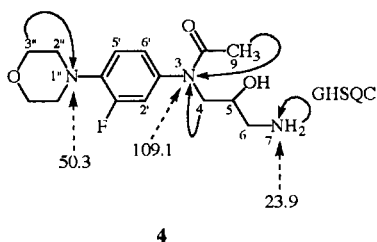
aralkyl N-3 nitrogen of **2**. The terminal amide nitrogen experienced a downfield shift of 4.2 ppm, and was observed at 109.5 ppm.

The long-range correlations observed for the first major degradant are shown by **2**. Strong and weak correlations are denoted by an (s) or (w), respectively. Again, all expected correlations were observed, and were similar to those observed for **1**.

#### 3-*N*-Acetyl Degradant (4).

Migration of the acetyl group, N-7  $\rightarrow$  N-3, presumably *via* the intermediacy of **3** as shown in Scheme 1, afforded the second major thermal degradant observed in studies of aqueous solutions of linezolid (**1**).

The  $^1\text{H}$  NMR spectrum of **4** exhibited a hydroxyl resonance at 5.45 ppm, and a two-proton terminal amine resonance at 7.67 ppm. The amide proton resonance observed in the proton spectrum of **2** was not observed in the proton spectrum of **4**. The *N*-acetyl methyl resonance chemical shifts of **2** and **4** were not diagnostically useful.



In the  $^1\text{H}$ - $^{15}\text{N}$  GHMBC spectrum of **4**, an amide  $^{15}\text{N}$  resonance was observed at 109.1 ppm, which does not differ appreciably from the N-7 amide resonance of **2** (109.5 ppm) or the oxazolidinone carbamate N-3 nitrogen resonance of **1** (105.3 ppm). The long-range  $^1\text{H}$ - $^{15}\text{N}$  correlations, however, establish that the amide nitrogen in question is located at N-3 rather than N-7 based on the correlations from the aromatic protons. These data, in conjunction with the molecular weight of the molecule and the acetyl methyl correlation to the nitrogen in question confirm the structure of **4**.

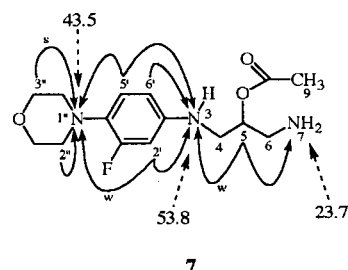
The long-range correlations for the second major degradant are shown by **4**. This sample underwent rapid facile degradation in solution, making the acquisition of long-range  $^1\text{H}$ - $^{15}\text{N}$  data difficult; as a result not all of the expected correlations were observed. The chemical shift of the terminal amino group, N-7, was obtained from a direct correlation  $^1\text{H}$ - $^{15}\text{N}$  GHSQC experiment. The long-range GHMBC exhibited two responses that were considered to be the strongest in the long-range  $^1\text{H}$ - $^{15}\text{N}$  GHMBC spectra of **1** and **2**. It was assumed that the free rotation of the aliphatic side chain of the molecule prevented the observation of correlations to N-7.

Relative to **2**, the N-3 resonance is shifted downfield by 52.4 ppm, consistent with acetylation. Interestingly, with the acetylation at N-3, the morpholine ring nitrogen again shifts downfield by 7.2 ppm to resonate at 50.3 ppm, vs. a chemical shift of 43.1 ppm for this nitrogen in **2**. This observation adds further credence to the argument that the chemical shift of the morpholine nitrogen is affected by the transmission of electronic effects from N-3 via the  $\pi$  electrons of the phenyl ring. Finally, the N-7 resonance exhibited the largest change of any of the nitrogen resonances of **4** shifting upfield by 85.6 ppm to 23.9 ppm consistent with the structural change from an amide to the corresponding primary amine.

#### O-5 Acetate Degradant (7).

The O-5 acetate degradant, **7**, can be considered a secondary degradation product requiring the migration of

the acetyl group from either N-7 following hydrolytic decarboxylation to afford **2** (pathway B) or from N-3 of **4**. Presumably, the formation of **7** from **2** occurs through the intermediacy of a specie such as **5**, or from **4** through an intermediate such as **6**. Neither **5** nor **6** have been either observed in solution or isolated. Moreover, **7** has only been observed in research stability studies in thermally degraded samples of **4**, and then only in very small quantities.



The  $^1\text{H}$  spectrum of **7** exhibited no hydroxyl resonance as observed for **2**. A one-proton resonance was observed at 5.77 ppm consistent with the anilino N-3 amine; a two-proton signal resonating at 7.81 ppm was also consistent with the N-7 terminal amine.

After the migration of the acetyl group to afford **7**, the N-3 resonance was observed at 53.8 ppm. This chemical shift of N-3 is slightly upfield of the N-3 shift of **2** (56.7 ppm) and considerably upfield of the corresponding N-3 chemical shifts of the parent molecule, **1**, and degradant **4**, for which the N-3 is an amide-like environment in both cases (93.8 and 104.6 ppm, respectively). The terminal amino nitrogen, N-7 resonated at 23.7 ppm and was relatively unchanged relative to the degradant **4**, in which the corresponding nitrogen resonated at 23.9 ppm. The N-3 resonance was considerably upfield relative to **1** and **2** as this position was amide-like in both of these molecules (105.3 and 109.5 ppm, respectively).

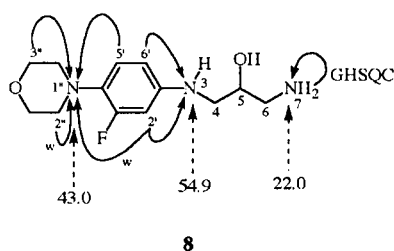
The morpholine nitrogen resonance of **7** was observed at 43.5 ppm, and was shifted upfield relative to the parent molecule, **1**, and degradant **4**, both of which have an amide-like environment at N-3 that can influence the chemical shift of the morpholine nitrogen via the intervening phenyl. Relative to **2** (43.1 ppm), the chemical shift of the morpholine nitrogen of **7** was essentially unchanged (43.5 ppm).

The long-range GHMBC correlations for the O-5 acetate degradant are shown by **7**. Expected correlations were observed. Of note, the acetate methyl did not exhibit a response, consistent with *O*-acetylation.

## Desacetyl Degradant (8).

The final degradant in the cascade, **8**, is formed *via* deacetylation. Presumably, any of the degradants following hydrolytic cleavage of the oxazolidine ring, **2**, **4**, or **7**, could directly undergo deacetylation to give **8**. The nitrogen chemical shifts of **8**, as would be expected, are virtually the same as those exhibited by **7**, as the electronic environments of the three nitrogens would be expected to differ only very little relative to the *O*-acetyl degradant.

The long-range correlations for the final degradation cascade product are shown on the structure. Weak correlations are denoted by a (w). Not all expected correlations were observed. The correlations from the phenyl and morpholino ring protons to N-1" and N-3 are as expected, but no responses were observed from the side chain protons to either N-3 or N-7. Again, the chemical shift for the terminal amine had to be obtained from a direct correlation GHSQC spectrum.



## Conclusion.

The assignment of the thermal degradant structures of linezolid (**1**) can be accomplished by conventional spectroscopic means when the exchangeable protons are observed in the proton reference spectra and when appropriate amide IR bands are also observed. In some cases, however, we have found that the exchangeable protons of some isolate samples are quite broad and not amenable to convenient analysis and structure assignment. In such cases, as shown in the present study, the combination of  $^{15}\text{N}$  chemical shift considerations in conjunction with the observed long-range couplings allows the unequivocal determination of the location of the acetyl group. For example, the N-3 and N-7 acetyl degradants, **2** and **4**, respectively, can be differentiated on the basis of the long-range couplings observed to each nitrogen. The  $^{15}\text{N}$  chemical shift for **2** are essentially the same as for **4**, although the long-range couplings to N-3 from the aromatic protons of **2** are not possible for **4**. These methods at moderately high observation frequencies (500 or 600 MHz) coupled with small format NMR probe designs (either 3 mm micro or 1.7 mm SMIDG

(submicro)) allow these studies to be performed on relatively modest sample quantities, down to ~ 1 mg [3]. While it is preferable to use more conventional techniques when possible, it is also beneficial to have a back-up method such as that described in this study available should the conventional approach fail for any reason.

## EXPERIMENTAL

Degradation products were obtained *via* thermally stressed samples of linezolid. The high temperature autoclave cycles were performed at various conditions to determine the proper degradation cascade and corresponding kinetics, which will be reported later.

The semi-preparative HPLC conditions employed a 20 x 250 mm, Kromasil C18 column with a gradient acetonitrile - aqueous trifluoroacetic acid (TFA) mobile phase. The pooled fractions were diluted with Milli-Q water and concentrated, desalted, and reduced in chemical noise-causing components *via* trapping on a 10 x 250 mm, YMC ODS AQ column. The eluent from the trapping column containing the peaks was freeze-dried to yield 0.5 to 1 mg each. The analytical HPLC purity of **3**, **4**, and **5** were 94, 91, and 98 %, respectively. Both **1** and **2** were obtained as pure samples.

High resolution mass spectrometry was performed on a Finnigan MAT-900ST mass spectrometer operating in the micro-ESI (micro electrospray ionization) mode. Accurate mass measurement was carried out by linear E-scan peak matching at a resolution of 11,000 ( $m/\Delta m$ , 10 % valley definition) for **2**, and 9,800 for **3**. Reference ions from PEG300;  $(\text{C}_2\text{H}_4\text{O})_6\text{H}_2\text{O}^+\text{Na}$  and  $(\text{C}_2\text{H}_4\text{O})_7\text{H}_2\text{O}^+\text{Na}$  at 305.15762 and 349.18384 Daltons were used to bracket the sample pseudo-molecular ions of the three isolates at 312 Daltons. The accurate mass measured for each of the three isomers were all within 1.9 ppm of the theoretical mass for their assigned structures.

ESI/MS/MS product ion spectra of the protonated molecular ion of each of the three isolates were recorded using a Finnigan TSQ-7000 triple quadrupole mass spectrometer. Several micrograms of each isolate were dissolved in 1:1 acetonitrile:water containing 2% acetic acid prior to TESI sample introduction. Product ion spectra were recorded using argon collision gas at an indicated pressure of 2 tor and collision energy of  $E_{\text{lab}}=40$  eV. Product ion spectra were recorded at unit mass resolution in the profile mode between 10 and 350 amu.

Reflectance micro-IR spectra for the degradation products were collected from 4000 to 650  $\text{cm}^{-1}$  on a Nicolet 760 FTIR equipped with a TGS detector. Sensitivity, expressed as instrument gain, was 4. Data were processed as a Fourier transform utilizing a Happ-Genzel apodization.

NMR samples were prepared in a glove box under a dry argon atmosphere. The degradants were dissolved in 120  $\mu\text{L}$  DMSO- $d_6$  (99.996% D, Cambridge Isotope Laboratories) and transferred to Wilmad 328 3mm micro NMR tubes. All  $^1\text{H}$  and  $^{13}\text{C}$  spectra were acquired on a Varian INOVA 400 spectrometer operating at a proton frequency of 399.08 MHz, and equipped with Nalorac Z•SPEC™ MIDTG and MIDG 3mm micro probes. Assignments were accomplished *via* the homonuclear TOCSY,  $^1\text{H}$ - $^{13}\text{C}$  GHSQC and GHMBC experiments, the latter optimized for an assumed 8 Hz long-range coupling [1].

Long-range  $^1\text{H}$ - $^{15}\text{N}$  GHMBC NMR experiments [4] were performed at natural abundance using a Varian INOVA 600 MHz, three channel NMR spectrometer with 28 channel Oxford shims, operating at a proton frequency of 599.75 MHz. The instrument was equipped with a Nalorac Z•SPEC<sup>™</sup> MIDTG-600-3 micro NMR probe for **1** and **2**. The 90° pulse calibrations were as follows: 7.30  $\mu\text{s}$  at 49 dB (63 max) for  $^1\text{H}$ , and 31.0  $\mu\text{s}$  at 57 dB (63 max) for  $^{15}\text{N}$ . The  $^1\text{J}_{\text{NH}}$  coupling delay in the low-pass J-filter was set to 90 Hz, and the long-range optimization ( $^n\text{J}_{\text{NH}}$ ) was set for 6 Hz.

The  $^{15}\text{N}$  chemical shift of *N*-phenylmorpholine used as a reference was measured at 60.2 ppm as a dimethyl- $\text{d}_6$  sulphoxide (99.996% D, CIL) solution. All chemical shifts are reported in ppm downfield of liquid ammonia, which was taken as 379.5 ppm upfield of nitromethane.

For degradants **4**, **7**, and **8**, the initial 120  $\mu\text{L}$  samples were spun to dryness, then were dissolved in 30  $\mu\text{L}$  dimethyl- $\text{d}_6$  sulphoxide (99.996% D, CIL) and transferred to a 1.7 mm NMR tube made in the laboratory from 1.7 mm o.d. precision glass tubing from Wilmad Co. A Nalorac

Z•SPEC<sup>™</sup> SMIDG<sup>™</sup>-600-1.7 (SMIDG, submicro inverse-detection gradient) NMR probe was then employed for the  $^1\text{H}$ - $^{15}\text{N}$  GHMBC data. The 90° pulse calibrations were as follows: 6.65  $\mu\text{s}$  at 49 dB (63 max) for  $^1\text{H}$ , and 21.2  $\mu\text{s}$  at 59 dB (63 max) for  $^{15}\text{N}$ . Pulses were calibrated using standard methods. The  $^1\text{J}_{\text{NH}}$  coupling delay in the low-pass J-filter was set to 90 Hz, and the long-range optimization ( $^n\text{J}_{\text{NH}}$ ) was set for 3.5 Hz for **4**, **7**, and **8**.

#### REFERENCES AND NOTES

- [1] A. Bax and S. Subramanian, *67*, 565 (1986); R. E. Hurd, and B. K. John, *J. Magn. Reson.*, **91**, 648 (1991).
- [2] K. A. Farley, P. B. Bowman, J. C. Brumfield, F. W. Crow, W. K. Duholke, J. E. Guido, R. H. Robins, S. M. Sims, R. F. Smith, T. J. Thamann, B. S. Vonderwell, and G. E. Martin, *Magn. Reson. Chem.*, **36**, S11 (1998).
- [3] C. E. Hadden and G. E. Martin, *J. Nat. Prod.*, **61**, 969 (1998).
- [4] Long-range  $^1\text{H}$ - $^{15}\text{N}$  heteronuclear shift correlation techniques have recently been reviewed: G. E. Martin and C. E. Hadden, *J. Nat. Prod.*, **63**, 543 (2000).